




ORIGINAL ARTICLE

De novo emergence of SARS-CoV-2 spike mutations in immunosuppressed patients

Lacy M. Simons^{1,2}  | Egon A. Ozer^{1,2} | Stephanie Gambut³ | Taylor J. Dean^{1,2} |
Li Zhang³ | Pavan Bhimalli³ | Jeffrey R. Schneider³  | João I. Mamede³ |
Michael G. Ison^{1,4}  | Reem Karmali^{5,6} | Leo I. Gordon⁵ | Ramon Lorenzo-Redondo^{1,2} |
Judd F. Hultquist^{1,2}

¹Department of Medicine, Division of Infectious Diseases, Northwestern University Feinberg School of Medicine, Chicago, Illinois, USA

²Center for Pathogen Genomics and Microbial Evolution, Northwestern University Havelly Institute for Global Health, Chicago, Illinois, USA

³Department of Microbial Pathogens and Immunity, Rush University Medical Center, Chicago, Illinois, USA

⁴Department of Surgery, Division of Organ Transplantation, Northwestern University Feinberg School of Medicine, Chicago, Illinois, USA

⁵Department of Medicine, Division of Hematology and Oncology, Northwestern University Feinberg School of Medicine, Chicago, Illinois, USA

⁶Robert H. Lurie Comprehensive Cancer Center, Chicago, Illinois, USA

Correspondence

Judd F. Hultquist, Department of Medicine, Division of Infectious Diseases, Northwestern University Feinberg School of Medicine, 303 E. Superior St., Chicago, IL 60611, USA.
Email: judd.hultquist@northwestern.edu

Lacy M. Simons and Egon A. Ozer contributed equally to this work.

Abstract

Background: The continuing evolution of severe acute respiratory syndrome coronavirus 2 (SARS-CoV-2) variants with decreased susceptibility to neutralizing antibodies is of clinical importance. Several spike mutations associated with immune escape have evolved independently in association with different variants of concern (VOCs). How and when these mutations arise is still unclear. We hypothesized that such mutations might arise in the context of persistent viral replication in immunosuppressed hosts.

Methods: Nasopharyngeal specimens were collected longitudinally from two immunosuppressed patients with persistent SARS-CoV-2 infection. Plasma was collected from these same patients late in disease course. SARS-CoV-2 whole genome sequencing was performed to assess the emergence and frequency of mutations over time. Select Spike mutations were assessed for their impact on viral entry and antibody neutralization in vitro.

Results: Our sequencing results revealed the intrahost emergence of spike mutations that are associated with circulating VOCs in both immunosuppressed patients (del241-243 and E484Q in one patient, and E484K in the other). These mutations decreased antibody-mediated neutralization of pseudotyped virus particles in cell culture, but also decreased efficiency of spike-mediated cell entry.

Conclusions: These observations demonstrate the de novo emergence of SARS-CoV-2 spike mutations with enhanced immune evasion in immunosuppressed patients with persistent infection. These data suggest one potential mechanism for the evolution of VOCs and emphasize the importance of continued efforts to develop antiviral drugs for suppression of viral replication in hospitalized settings.

KEYWORDS

COVID-19, immunosuppressed, persistent infection, SARS-CoV-2, spike mutation, variants of concern, viral evolution

This is an open access article under the terms of the [Creative Commons Attribution-NonCommercial-NoDerivs](https://creativecommons.org/licenses/by-nc-nd/4.0/) License, which permits use and distribution in any medium, provided the original work is properly cited, the use is non-commercial and no modifications or adaptations are made.

© 2022 The Authors. *Transplant Infectious Disease* published by Wiley Periodicals LLC.



1 | INTRODUCTION

Specific genetic changes in SARS-CoV-2 have been associated with clinically relevant features including increased transmission, resistance to therapeutics, impaired diagnostic detection, and/or immune escape.¹⁻⁴ Understanding the mechanisms behind the emergence of SARS-CoV-2 variants of concern (VOCs) with these features is key to developing strategies to prevent their further appearance and expansion. Several evolutionarily distinct VOCs share identical nonsynonymous mutations in their spike open reading frames, despite arising from distinct ancestral lineages.^{5,6} This sudden accumulation of consequential mutations and several examples of convergent evolution in VOCs suggest that discrete selective pressures underlie the appearance of these variants. One hypothesis to explain VOC emergence is the accumulation of mutations that increase viral fitness within individuals with prolonged infections and subsequent transmission to and expansion in the population.⁷⁻⁹

Here, we report two cases of immunosuppressed individuals (Patient A and Patient B), each with persistent SARS-CoV-2 infection in whom the viral populations convergently acquired mutations associated with circulating VOCs. Persistent infection in this context is defined by a continual or intermittent display of symptoms following a positive diagnostic test for SARS-CoV-2 for a time period of 30 days or greater. We find that both persistently infected patients in this study exhibited increases in intrahost viral population diversity over the course of infection that ultimately resulted in the emergence of a new, dominant genotype. These results demonstrate the potential for concerning variants to evolve in patients with persistent SARS-CoV-2 infection and support the call increased viral surveillance in immunosuppressed patients over long disease courses. The potential for SARS-CoV-2 to evolve in cases of persistent infection also has implications for infection prevention measures in the community and in hospital settings and emphasizes the importance of ongoing efforts to develop effective antiviral drugs for the suppression of viral replication.

2 | METHODS

2.1 | Clinical data extraction

Electronic chart review was carried out to extract and compile the following clinical data elements per study protocol STU00212267: presentation, laboratory/radiographic findings, treatments, co-morbidities, and outcomes of COVID-19.

2.2 | Specimen collection

Residual nasopharyngeal swab specimens from each patient were collected from Northwestern Memorial Hospital's Clinical Microbiology Laboratory following SARS-CoV-2 diagnostic testing per study protocol STU00212260 (as in Lorenzo-Redondo et al.¹⁰). Both patients also provided informed consent for study staff to collect addi-

tional nasopharyngeal swabs and whole blood per study protocol STU00206652. Nasopharyngeal swabs were stored in Viral Transport Media, inactivated by incubation at 60°C for 1 h and frozen in 1 ml aliquots at -80°C. Whole blood was collected from study participants in Vacutainer CPT mononuclear cell preparation tubes containing sodium heparin (Becton Dickinson). Plasma was removed, pooled, and frozen in 1 ml aliquots at -80°C. Peripheral blood mononuclear cells were removed, washed with 1x PBS containing 0.5% BSA and 2mM EDTA, and frozen in cryopreservation media (1x FBS, 10% DMSO) at -80°C.

2.3 | Viral load determination

Viral RNA was extracted from nasopharyngeal specimens utilizing the QIAamp Viral RNA Minikit (Qiagen). Laboratory testing for SARS-CoV-2 presence was performed by quantitative reverse transcription and polymerase chain reaction (PCR) with the CDC 2019-nCoV RT-PCR Diagnostic Panel utilizing N1 and RNase P probes and positive control plasmids for standard curve determination (Integrated DNA Technologies) as previously described.¹¹

2.4 | Whole genome sequencing from Viral RNA

cDNA synthesis was performed with SuperScript IV First Strand Synthesis Kit (Thermo) using random hexamer primers according to manufacturer's specifications. Direct amplification of viral genome cDNA was performed as previously described using the Artic Network version 4 primers.¹² Sequencing library preparation of genome amplicon pools was performed using the SeqWell plexWell 384 kit per manufacturer's instructions. Pooled libraries were sequenced on the Illumina MiSeq using the V2 500 cycle kit. Sequencing reads were trimmed to remove adapters and low-quality sequences using Trimmomatic v0.36. Trimmed reads were aligned to the reference genome sequence of SARS-CoV-2 (accession MN908947.3) using bwa v0.7.15. Pileups were generated from the alignment using samtools v1.9 and consensus sequence determined using iVar v1.2.2 with a minimum depth of 10, a minimum base quality score of 20, and a consensus frequency threshold of 0 (i.e., majority base as the consensus). Each viral specimen underwent repeated library preparation and sequencing on at least 2 separate days with pooling of sequence reads prior to analysis to increase overall coverage and read depth.

2.5 | Phylogenetic and diversity analysis

We used Nextclade (<https://clades.nextstrain.org/>) to classify viral clades. Genome sequences were aligned using MAFFT v7.453 software and a Maximum Likelihood (ML) phylogeny was inferred with IQ-Tree v2.0.5 using the SARS-CoV-2 reference genome Wuhan-Hu-1 (NC_045512) to root the tree as in.¹⁰ TreeTime v0.7.6 was used to estimate time scaled phylogeny using the previously inferred ML

phylogeny. Additionally, we performed phylogenetic analysis of the two patients' sequences in the context of the broader Chicago epidemic, using all Chicago sequences submitted by our laboratory to GISAID (GISAID.org) between December 2020 and June 2021. We generated diversity phylogenetic trees and analyzed genetic clustering of the patients' longitudinal sequences using the same approach as above (i.e., MAFFT v7.453 alignment followed by IQ-Tree v2.0.5 ML tree inference). Shannon Entropy was calculated using the nucleotide frequencies obtained from iVar applying the formula: $Sh = -\sum [-(p_i) \cdot \log_2(p_i)]$; where Sh is Shannon Entropy calculated for each position, and p_i is the frequency of each nucleotide in each position.¹³ To ensure a robust estimation of diversity, Shannon Entropy calculations were limited to positions with a minimum read depth of 1000 reads and a minimum frequency of 0.01 for minority variant calling. For calling of minority variants in the spike gene, a minimum read depth of 50 reads, and a minimum frequency of 0.3 was used.

2.6 | Antibody quantification

Antibody titers for Spike N-terminal domain (NTD) and receptor binding domain (RBD) were determined by ELISA as previously described using His-RBD and NTD antigens (Acro Biosystems) and Ni-NTA HisSorb ELISA plates (Qiagen).¹⁴ Anti-RBD antibody CR3022 (Creative Biolabs) and Anti-NTD antibody SPD-M121 (Acro Biosystems) were used to construct standard curves.

2.7 | Spike expression constructs

Oligonucleotides carrying the E484K, E484Q, and del241-248 mutations were used to perform site-directed mutagenesis of the pCAGGS-Spike SARS-CoV-2 plasmid (B.1 Spike; BEI resources). Successful mutagenesis was confirmed by Sanger sequencing.

2.8 | Viral entry and neutralization assays

Pseudotyped viruses were constructed for use in viral entry and neutralization assays as in Schmidt et al.¹⁵ Spike expression constructs carrying the E484K and E484Q with and without the 241-248 deletion were used to generate replication-incompetent, HIV-based (pNL4-3-nanoluc Δ env), luciferase reporter viruses pseudotyped with each Spike protein. For cell entry assays, the viruses were normalized to the amount of HIV capsid protein (p24) and used to challenge HeLa-ACE2 cells at several dilutions as described.¹⁶ HeLa-Ace2 cells were generated by lentiviral transduction and puromycin selection of parental cells (ATCC HeLa CCL-2) with RRL.sin.cPPT.SFFV/Ace2.IRES-puro.WPRE (MT126) (Addgene #145839). Neutralization assays were performed similarly, but HeLa-Ace2 cells were first preincubated with serial dilutions of patient sera and then challenged with the pseudotyped viruses for 48-h. Reporter gene expression was determined downstream of both assays using the Nano-Glo Dual-Luciferase

Reporter Assay (Promega). To test for differences in neutralization, we fit a linear mixed effects model that included serum concentration, virus genotype, and the interaction of both variables controlling for the different replicates performed using the nlme package in R v4.0.3. Subsequently, we tested all pairwise comparisons between mutants within the fitted model and adjusted for multiple comparisons using Tukey's method. Comparisons with an adjusted p -value $<.05$ were considered significantly different. For this estimation, we used the luminescence values measured in relative light units (RLUs) normalized by average RLU values of the 'no plasma' controls.

2.9 | Patient histories

Patient A was a 64-year-old man with a medical history of mantle cell lymphoma diagnosed in 2017. After several rounds of chemotherapy, the patient underwent autologous hematopoietic stem cell transplantation in August of 2020. The patient was scheduled to receive rituximab every 2 months for maintenance and had received two doses by December 2020. He received his first SARS-CoV-2 Pfizer-BNT-162b2 vaccination on December 23, 2020. Five days later he developed fever and cough. On January 5, 2021, he tested positive for SARS-CoV-2 by polymerase chain reaction (Cepheid Flu/RSV/SARS-CoV-2). Further rituximab doses were held, and he received bamlanivimab on January 6, 2021. He developed worsening shortness of breath, bilateral ground glass changes on chest radiograph, and was started on outpatient prednisone on January 26, 2021. He was subsequently admitted to the hospital with radiologic and clinical progression and started on remdesivir. He progressed to acute respiratory distress syndrome (ARDS), requiring intubation a week later and subsequently transitioned to venovenous extracorporeal membrane oxygenation (ECMO). Dexamethasone was administered on February 26, 2021. His course was complicated by multiple healthcare-associated pneumonias, pneumothoracies, and bleeding from the ECMO site. He was deemed not to be a transplant candidate and died 7 months after his initial COVID-19 diagnosis.

Patient B was a 48-year-old man with past medical history of chronic lymphocytic leukemia with Richter's transformation initially diagnosed in March 2019. After initial rounds of chemotherapy, including rituximab, his lymphoma went into remission. The patient had recurrence of his lymphoma in November 2020 and was started on venetoclax, ubituximab, and umbralisib in clinical trial in January 2021. The patient then developed symptoms of fatigue, fevers and myalgias without loss of taste or smell, and subsequently tested positive for SARS-CoV-2 by PCR on March 4, 2021. Chemotherapy was temporarily held, and he received a single dose of bamlanivimab on March 5, 2021. Symptoms transiently improved, and he tested negative for SARS-CoV-2 on April 26, 2021 after which time chemotherapy was resumed. Mild respiratory symptoms persisted intermittently until June 17, 2021 when a low-grade fever, shortness of breath, and worsening upper respiratory tract symptoms prompted further evaluation. A chest computed tomography (CT) scan revealed diffuse bilateral lower lung ground glass opacities, consistent with COVID-19. The patient



subsequently tested positive for SARS-CoV-2 from bronchioalveolar lavage sampling. After exhibiting worsening symptoms, the patient was admitted to the hospital on June 25, 2021, at which time he was administered remdesivir and a single, compassionate-use dose of casirivimab-indecimab. The patient had no significant hypoxemia and did not receive corticosteroid therapy. Fever subsided and respiratory symptoms improved with treatment. A repeat chest CT revealed resolution of ground glass changes; the patient was discharged following resolution of all clinical symptoms on July 4, 2021. At the time of this study, the patient had not received any vaccine doses for SARS-CoV-2.

3 | RESULTS

Each patient underwent multiple PCR-based tests for SARS-CoV-2 over the course of their hospitalizations as depicted in Figure 1A. Over the span of 130 days, nine of nine (100%) diagnostic SARS-CoV-2 PCR tests were positive for patient A with an average N1 Ct value of 29.02 (range 23.18–36.17). Over the span of 117 days, two of five (40%) diagnostic SARS-CoV-2 PCR tests were positive for patient B with an average N1 Ct Value of 26.95 (range 22.76–31.14) (Figure 1B).

Viral whole genome sequences were successfully assembled for five of the nine positive specimens (55%) from patient A and for both of the positive specimens (100%) from patient B. The average read depth across the sequences ranged from 619 to 3795 reads per position. Within spike, the average read depth ranged from 539 to 2631 reads per position. The consensus sequence of each viral genome assembly for patient A mapped to Clade 20B, while the consensus sequence of each viral genome assembly for patient B mapped to Clade 20G. Consensus sequences were deposited to the GISAID database (Patient A sequences 1–5: EPI_ISL_1501693, EPI_ISL_1501684, EPI_ISL_12599131, EPI_ISL_2372953, EPI_ISL_2372989; Patient B sequences 1–2: EPI_ISL_3185852 and EPI_ISL_3185853).

Patient A tested consistently positive by PCR, had ongoing respiratory symptoms, and showed infection with the same 20B sublineage at each timepoint, all suggestive of persistent infection. Patient B had transient improvement in symptoms coinciding with a negative PCR-based test result but had persistent respiratory symptoms. The sequencing data revealed infection with the same 20G sublineage at each timepoint, again consistent with persistent infection. Note that while 20G was circulating in the Chicago area with 37% frequency when the patient was first diagnosed in early March 2021, it was circulating with less than 1% frequency by mid-June of that year at the time of second sampling, making reinfection highly unlikely (<https://outbreak.info/>, accessed May 9, 2022). To confirm that each case most likely reflected a persistent infection, the SARS-CoV-2 whole genome sequences from each patient were assembled in a phylogenetic tree with all other available SARS-CoV-2 whole genome sequences from clinical isolates collected at Northwestern Memorial Hospital between December of 2020 and June of 2021 (Figure 2A). Patient A sequences (blue) cluster together with 98% support by approximate likelihood-ratio test (aLRT) and 100% support by bootstrap. Patient A sequences (red) cluster together with 93.5% support by aLRT and 100% support

by bootstrap. Taken together, the clinical histories and sequence analyses strongly suggest persistent, long-term infection of both patients with SARS-CoV-2.

While consensus sequences mapped within the same sublineage over time, de novo mutations arose in each patient over the course of infection, several of which became dominant at later timepoints (Figure 2B). Consistent with the emergence of new mutations, intra-host viral diversity, measured as the Shannon entropy in each specimen, was also observed to increase over time (Figure 2C). These changes included a number of mutations in the viral spike protein (Figure 2D). In patient A, this included a 7 amino acid deletion in Spike between positions 241–248, and a similar 3 amino acid deletion between positions 241–243 that became more prevalent at later time points. De novo emergence of the 241–243 deletion in spike is notable as this same mutation is observed in the Beta VOC (Figure 2E). The viral isolate in patient A also developed a spike E484Q mutation, which was observed in formerly monitored variant Kappa. Patient B developed a similar E484K mutation, previously observed in the Beta and Gamma VOCs as well as in several formerly monitored variants (Figure 2D,E). The Spike 241–243 deletion and the E484K mutation have been previously linked with escape from neutralizing antibodies.^{2,5,17–19}

Both patients received the spike-targeting monoclonal antibody therapeutic bamlanivimab early in their treatment course (Figure 1A). To determine if either patient had later developed antibodies against SARS-CoV-2 Spike, blood samples were taken from patients A and B 94 and 114 days after symptom onset (85 and 112 days after bamlanivimab treatment), respectively. Antibody levels against the NTD and RBD of spike were quantified by enzyme-linked immunoassay (ELISA). Plasma collected from a fully vaccinated, immunocompetent individual was used as a positive control. Patient A showed detectable levels of antibody against Spike NTD (24.60 µg/ml), but no detectable antibodies against the RBD. Patient B showed no detectable levels of antibody against spike NTD or RBD (Figure 3A).

Given that some of the emergent spike variants have been previously linked to increased antibody escape (241–243 deletion and E484K mutation),^{2,5} we wanted to determine if the other observed mutations in these patients conferred similar phenotypes. To test this, the wild-type, parental spike protein from these clades (B.1 lineage) was cloned into a mammalian expression construct. The E484Q and E484K variants with and without the 241–248 deletion from patient A were subsequently cloned and used to generate replication-incompetent, HIV-based, luciferase reporter viruses pseudotyped with each Spike protein. Viruses were normalized to the amount of HIV capsid protein (p24) and used to challenge HeLa-ACE2 cells in cell culture at several dosages. Each mutation was observed to negatively impact viral fusion as measured by luciferase reporter activity in this assay, with the E484 mutations causing minor defects and the spike deletion causing a dominant, larger defect (Figure 3B).

To determine if these mutations conferred enhanced antibody escape, a subset of these viruses (wild-type, E484Q, 241–248 deletion, and E484Q+241–248 deletion) were incubated with a dilution series of plasma from patient A. While both the E484Q and del241–248 mutations alone showed limited changes in the ability of the pseudotyped

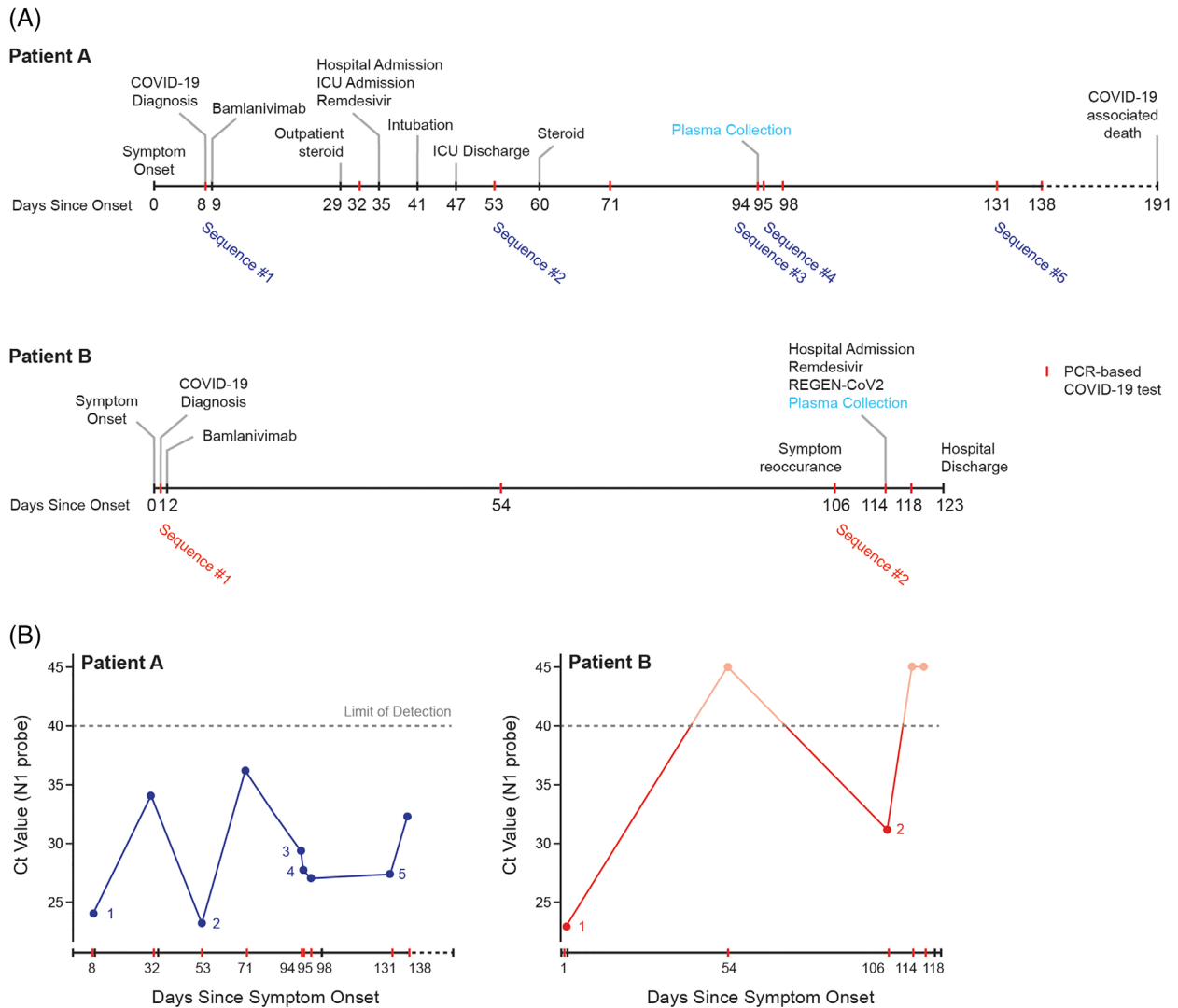


FIGURE 1 Histories of patients A and B with persistent severe acute respiratory syndrome coronavirus 2 (SARS-CoV-2) infection. Panel A summarizes the clinical progression of two immunosuppressed patients starting at the time of COVID-19 symptom onset. Red tick marks represent dates of polymerase chain reaction (PCR)-based SARS-CoV-2 diagnostic testing. The date of plasma collection from each patient is indicated in light blue. Panel B shows the cycle threshold (Ct) value of the diagnostic SARS-CoV-2 PCR-based tests administered during each patient's clinical course. Dates of collection for SARS-CoV-2 isolates that successfully underwent whole genome sequencing are annotated with numbers. Specimens with Ct values beyond the limit of detection of 40 were artificially represented by points at 45.

viruses to evade antibody neutralization relative to the wild-type Spike protein, the E484Q+del241-248 double mutant virus was more resistant than either single mutant alone and showed significantly lower neutralization compared to wild type virus (adjusted p -value = .0483) (Figure 3C).

4 | DISCUSSION

This study documents de novo emergence of spike mutations in two immunosuppressed patients with persistent SARS-CoV-2 infection. Both patients tested serially positive for SARS-CoV-2 by PCR-based diagnostic testing, even beyond 100 days from symptom onset. Each patient was treated early in the course of their infections with the

monoclonal antibody therapeutic bamlanivimab and were later treated with remdesivir. Only one of the two patients developed detectable levels of anti-NTD spike antibodies in their blood. Viral whole genome sequencing revealed the accumulation of intrahost viral diversity over time, and the emergence of several de novo mutations. A number of these mutations mapped to the spike protein and were identical to mutations previously documented in VOC. In vitro characterization demonstrated that these mutations decreased viral entry efficiency but enhanced escape from neutralizing antibodies developed by the patient.

These results suggest that persistent SARS-CoV-2 replication in immunocompromised hosts can drive increased levels of intrahost viral diversity and apply selective pressure yielding viruses with fitness advantages.^{7,8,17} The Spike mutations examined in cell culture all

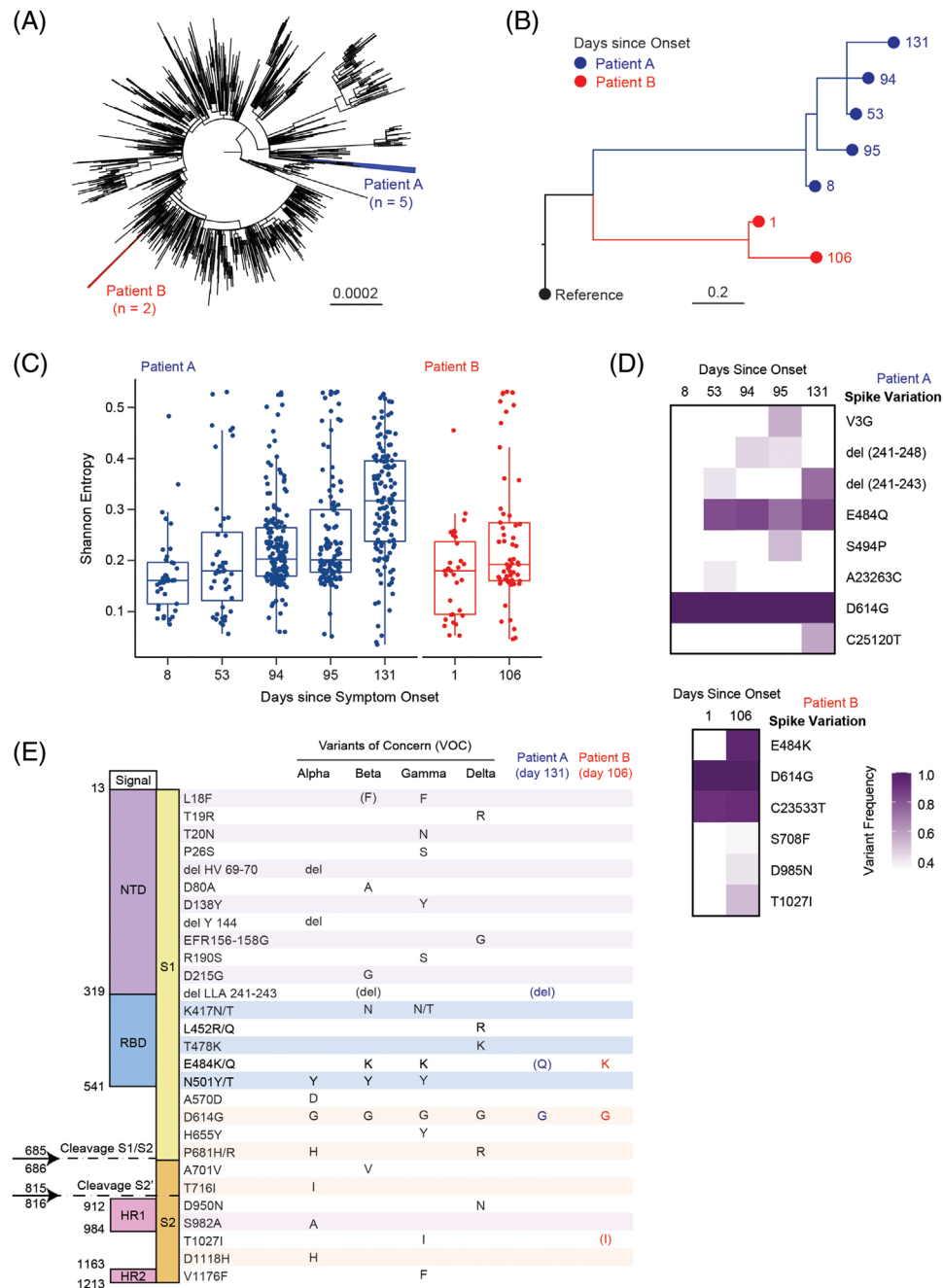


FIGURE 2 Intrahost emergence of spike mutations in severe acute respiratory syndrome coronavirus 2 (SARS-CoV-2) isolates from immunosuppressed patients. Panel A shows a phylogenetic tree of the consensus SARS-CoV-2 whole genome sequences from patient A (blue, five sequences) and patient B (red, two sequences) alongside all other available SARS-CoV-2 whole genome sequences from Northwestern Memorial Hospital collected between December 2020 and June 2021. Panel B shows a temporal phylogenetic tree comparing consensus SARS-CoV-2 whole genome sequences from patient A and patient B. The time since symptom onset of isolate collection is indicated to the right of each node. The SARS-CoV-2 reference genome Wuhan-Hu-1 (NC_045512) was used to root the tree. Panel C depicts one measure of viral diversity (Shannon entropy) calculated for each sequenced isolate labeled by the collection time since symptom onset. Each dot represents the Shannon entropy at a given nucleotide; the box-and-whisker plot reflects the median and interquartile range. Panel D shows a heat map of spike variant frequency found in each viral isolate. Only variants that achieved at least 30% frequency in at least one sample are shown. Panel E summarizes the Spike mutations found in four variants of concern (Alpha, Beta, Delta, and Gamma) and in the SARS-CoV-2 isolates from each patient at the time of last sampling.

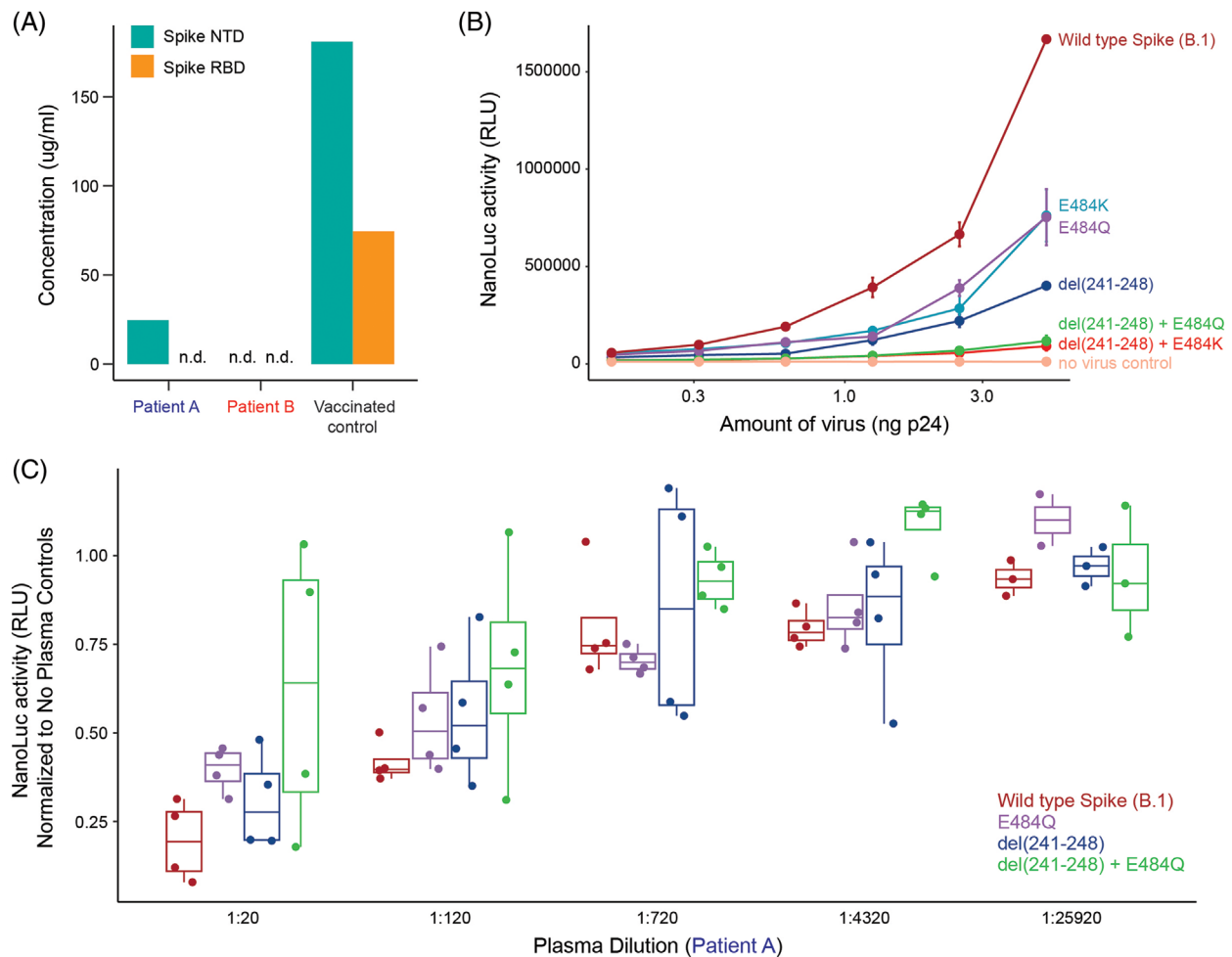


FIGURE 3 Emergent spike mutations confer decreased viral infectivity, but enhanced escape from antibody neutralization. Panel A depicts the levels of anti-spike antibodies targeting the N-terminal domain (NTD) or receptor-binding domain (RBD) in plasma collected from each patient or a fully vaccinated control subject (n.d. = not detectable). Panel B depicts luciferase activity in cells after *in vitro* challenge with reporter viruses pseudotyped with severe acute respiratory syndrome coronavirus 2 (SARS-CoV-2) spike proteins containing the indicated mutations. Each point reflects the average \pm standard deviation of two independent technical replicates. Panel C depicts the nanoluc luminescence signal in HeLa-ACE2 cells after challenge with reporter viruses pseudotyped with SARS-CoV-2 spike proteins containing the indicated mutations. The viruses were incubated with the indicated dilutions of plasma from Patient A prior to challenge, and the data are normalized to the no plasma control. Results are shown for four independent technical replicates (dots) with a box-and-whisker plot overlay reflecting the median \pm the interquartile range.

decreased viral entry efficiency but enhanced escape from neutralizing antibodies. It is unclear if this selection is driven by low levels of native antibody response in these hosts or by administration of monoclonal therapeutics like bamlanivimab. On the one hand, both patients developed E484 mutations in spike RBD that confer resistance to bamlanivimab, consistent with observations from other studies.^{17–20} On the other, a detectable anti-spike NTD antibody response did develop in one patient whose virus subsequently evolved deletions in the previously described antigenic supersite of the Spike NTD that were protective against neutralization by patient sera.²¹ If low levels of a native antibody response do contribute to the emergence of resistance mutations, the degree to which an individual is immunocompromised is likely to be a critical factor; sufficient antibody levels must be present to apply a selective pressure, but they also must be low enough to allow ongoing replication.

It is likely that both sources of antibody (therapeutic and host-derived) can drive viral selection, emphasizing the need to limit viral replication and viral diversity in patients with persistent infection through the development and administration of effective antivirals. The finding that several of the Spike mutations documented here mimic those previously observed in other VOCs suggest one potential origin for new variants with divergent spike proteins.^{6,22,23} While this study is limited to two patients within a single institution, intrahost emergence of the E484K spike mutation has also been recently documented in other patients who received bamlanivimab at other institutions, suggesting an important role of therapeutics in driving viral evolution.^{9,17,24,25} It is still unknown if intrahost selective pressures can also lead to the selection of viruses with enhanced transmissibility, or if enhancement of intrahost replication always results in a fitness cost to transmissibility. More studies in immunosuppressed and



immunocompromised hosts with persistent SARS-CoV-2 infection are needed to better understand and predict the ongoing evolution of this virus.

ACKNOWLEDGMENTS

Supported by grants (R21 AI163912, to Dr. Hultquist, U19 AI135964, to Dr. Ozer) from the National Institutes of Health; a grant (to Dr. Lorenzo-Redondo) from the Northwestern University Havey Institute for Global Health; a pilot award (to Dr. Ison) from the Northwestern University Clinical and Translational Science Institute; an internal award (to Dr. Mamede) from Rush University; and by grants (SCI16 and 21-00147, to Dr. Schneider) from the Walder Foundation's Chicago Coronavirus Assessment Network. This research was supported in part through the computational resources and staff contributions provided for the Quest high performance computing facility at Northwestern University, which is jointly supported by the Office of the Provost, the Office for Research, and Northwestern University Information Technology. Clinical data collection was supported in part by the Northwestern Medicine Enterprise Data Warehouse. The funding sources had no role in the study design, data collection, analysis, interpretation, or writing of the report.

CONFLICT OF INTEREST

M.G.I. has received research support, paid to Northwestern University, from AiCuris, GlaxoSmithKline Janssen and Shire. M.G.I. is a paid consultant for Adagio, AlloVir, Celltrion, Cidara, Genentech, Roche, Janssen, Shionogi, Takeda, Viracor Eurofins. M.G.I. is a paid member of the data and safety monitoring board (DSMBs) from CSL Behring, Janssen, Merck, SAB Biotherapeutics, Sequiris, and Takeda. R.K. has received research support, paid to Northwestern University, from BMS, Kite/Gilead, Viracta, and Takeda, served on Advisory Boards for BeiGene, Genentech, Roche, BMS, Kite/Gilead, EUSA, Karyopharm, Janssen, Epizyme and Morphosys and served on the Speakers Bureau for BeiGene, Kite/Gilead, AstraZeneca and Morphosys. All other authors declare no conflict of interest.

ORCID

Lacy M. Simons  <https://orcid.org/0000-0003-4041-6775>

Jeffrey R. Schneider  <https://orcid.org/0000-0001-9091-7653>

Michael G. Ison  <https://orcid.org/0000-0003-3347-9671>

REFERENCES

- Plante JA, Liu Y, Liu J, et al. Spike mutation D614G alters SARS-CoV-2 fitness. *Nature*. 2021;592(7852):116-121. <https://doi.org/10.1038/s41586-020-2895-3>
- Weisblum Y, Schmidt F, Zhang F, et al. Escape from neutralizing antibodies by SARS-CoV-2 spike protein variants. *Elife*. 2020;9:e61312. <https://doi.org/10.7554/eLife.61312>
- Greaney AJ, Starr TN, Gilchuk P, et al. Complete mapping of mutations to the SARS-CoV-2 spike receptor-binding domain that escape antibody recognition. *Cell Host Microbe*. 2021;29(1):44-57.e9. <https://doi.org/10.1016/j.chom.2020.11.007>
- Liu H, Yuan M, Huang D, et al. A combination of cross-neutralizing antibodies synergizes to prevent SARS-CoV-2 and SARS-CoV pseudovirus infection. *Cell Host Microbe*. 2021;29(5):806-818.e6. <https://doi.org/10.1016/j.chom.2021.04.005>
- McCarthy KR, Rennick LJ, Nambulli S, et al. Recurrent deletions in the SARS-CoV-2 spike glycoprotein drive antibody escape. *Science*. 2021;371(6534):1139-1142. <https://doi.org/10.1126/science.abf6950>
- Harvey WT, Carabelli AM, Jackson B, et al. SARS-CoV-2 variants, spike mutations and immune escape. *Nat Rev Microbiol*. 2021;19(7):409-424. <https://doi.org/10.1038/s41579-021-00573-0>
- Corey L, Beyrer C, Cohen MS, Michael NL, Bedford T, Rolland M. SARS-CoV-2 variants in patients with immunosuppression. *N Engl J Med*. 2021;385(6):562-566. <https://doi.org/10.1056/NEJMs2104756>
- Choi B, Choudhary MC, Regan J, et al. Persistence and evolution of SARS-CoV-2 in an immunocompromised host. *N Engl J Med*. 2020;383(23):2291-2293. <https://doi.org/10.1056/NEJMc2031364>
- Sabin AP, Richmond CS, Kenny PA. Emergence and onward transmission of a SARS-CoV-2 E484K variant among household contacts of a bamlanivimab-treated patient. *Diagn Microbiol Infect Dis*. 2022;103(1):115656. <https://doi.org/10.1016/j.diagmicrobio.2022.115656>
- Lorenzo-Redondo R, Nam HH, Roberts SC, et al. A clade of SARS-CoV-2 viruses associated with lower viral loads in patient upper airways. *EBioMedicine*. 2020;62:103112. <https://doi.org/10.1016/j.ebiom.2020.103112>
- Research use only 2019-novel coronavirus (2019-nCoV) real-time RT-PCR primers and probes. Centers for Disease Control and Prevention. Accessed June 6, 2020. <https://www.cdc.gov/coronavirus/2019-ncov/lab/rt-pcr-panel-primer-probes.html>
- Artic Network. SARS-CoV-2. Updates. <https://artic.network/ncov-2019>. Accessed June 21, 2021.
- Gregori J, Perales C, Rodriguez-Frias F, Esteban JI, Quer J, Domingo E. Viral quasispecies complexity measures. *Virology*. 2016;493:227-237. <https://doi.org/10.1016/j.virol.2016.03.017>
- Amanat F, Stadlbauer D, Strohmeier S, et al. A serological assay to detect SARS-CoV-2 seroconversion in humans. *Nat Med*. 2020;26(7):1033-1036. <https://doi.org/10.1038/s41591-020-0913-5>
- Schmidt F, Weisblum Y, Muecksch F, et al. Measuring SARS-CoV-2 neutralizing antibody activity using pseudotyped and chimeric viruses. *J Exp Med*. 2020;217(11):e20201181. <https://doi.org/10.1084/jem.20201181>
- Ozer EA, Simons LM, Adewumi OM, et al. Multiple expansions of globally uncommon SARS-CoV-2 lineages in Nigeria. *Nat Commun*. 2022;13(1):688. <https://doi.org/10.1038/s41467-022-28317-5>
- Jensen B, Luebke N, Feldt T, et al. Emergence of the E484K mutation in SARS-COV-2-infected immunocompromised patients treated with bamlanivimab in Germany. *Lancet Reg Health Eur*. 2021;8:100164. <https://doi.org/10.1016/j.lanepe.2021.100164>
- Lohr B, Niemann D, Verheyen J. Bamlanivimab treatment leads to rapid selection of immune escape variant carrying E484K mutation in a B.1.1.7 infected and immunosuppressed patient. *Clin Infect Dis*. 2021;73(11):2144-2145. <https://doi.org/10.1093/cid/ciab392>
- Pommeret F, Colomba J, Bigenwald C, et al. Bamlanivimab + etesevimab therapy induces SARS-CoV-2 immune escape mutations and secondary clinical deterioration in COVID-19 patients with B-cell malignancies. *Ann Oncol*. 2021;32(11):1445-1447. <https://doi.org/10.1016/j.annonc.2021.07.015>
- Destras G, Assaad S, Bal A, et al. Bamlanivimab as monotherapy in two immunocompromised patients with COVID-19. *Lancet Microbe*. 2021;2(9):e424. [https://doi.org/10.1016/S2666-5247\(21\)00189-0](https://doi.org/10.1016/S2666-5247(21)00189-0)
- McCallum M, De Marco A, Lempp FA, et al. N-terminal domain antigenic mapping reveals a site of vulnerability for SARS-CoV-2. *Cell*. 2021;184(9):2332-2347 e16. <https://doi.org/10.1016/j.cell.2021.03.028>



22. Deng X, Evdokimova M, O'Brien A, et al. Breakthrough infections with multiple lineages of SARS-CoV-2 variants reveals continued risk of severe disease in immunosuppressed patients. *Viruses*. 2021;13(9):1743. <https://doi.org/10.3390/v13091743>
23. Clark SA, Clark LE, Pan J, et al. SARS-CoV-2 evolution in an immunocompromised host reveals shared neutralization escape mechanisms. *Cell*. 2021;184(10):2605-2617.e18. <https://doi.org/10.1016/j.cell.2021.03.027>
24. Guigon A, Faure E, Lemaire C, et al. Emergence of Q493R mutation in SARS-CoV-2 spike protein during bamlanivimab/etesevimab treatment and resistance to viral clearance. *J Infect*. 2022;84(2):248-288. <https://doi.org/10.1016/j.jinf.2021.08.033>
25. Peiffer-Smadja N, Bridier-Nahmias A, Ferre VM, et al. Emergence of E484K mutation following bamlanivimab monotherapy among high-risk patients infected with the alpha variant of SARS-CoV-2. *Viruses*. 2021;13(8):1642. <https://doi.org/10.3390/v13081642>

How to cite this article: Simons LM, Ozer EA, Gambut S, et al. De novo emergence of SARS-CoV-2 spike mutations in immunosuppressed patients. *Transpl Infect Dis*. 2022:e13914. <https://doi.org/10.1111/tid.13914>